The pro-apoptotic activity of a vertebrate Bar-like homeobox gene plays a key role in patterning the *Xenopus* neural plate by limiting the number of *chordin*- and *shh*-expressing cells

Nicolas Offner[1,*], Nathalie Duval[1,*], Milan Jamrich[2] and Béatrice Durand[1,†]

[1]Unité Rétrovirus et Transfert Génétique, INSERM (U622). Institut Pasteur, 28, rue du Dr Roux, Paris 75015, France
[2]Department of Molecular and Cellular Biology, Baylor College of Medicine One Baylor Plaza, Houston, TX 77030, USA
*These authors contributed equally to this work
†Author for correspondence (e-mail: bdurand@pasteur.fr)

Accepted 25 January 2005

Development 132, 1807-1818
Published by The Company of Biologists 2005
doi:10.1242/dev.01712

Summary

Targeted disruption of effectors molecules of the apoptotic pathway have demonstrated the occurrence and magnitude of early programmed cell death (EPCD), a form of apoptosis that affects proliferating and newly differentiated cells in vertebrates, and most dramatically cells of the central nervous system (CNS). Little is known about the molecular pathways controlling apoptosis at these early developmental stages, as the roles of EPCD during patterning of the developing nervous system. We describe a new function, in *Xenopus* neurodevelopment, for a highly conserved homeodomain protein Barhl2. Barhl2 promotes apoptosis in the *Xenopus* neuroectoderm and mesoderm, acting as a transcriptional repressor, through a mechanism that cannot be attributed to an unspecific cellular stress response. We show that the pro-apoptotic activity of Barhl2 is essential during normal neural plate formation as it limits the number of *chordin*- and *Xshh*-expressing cells in the prospective notochord and floorplate, which act as organizing centers. Our findings show that *Barhl2* is part of a pathway regulating EPCD. They also provide evidence that apoptosis plays an important role in regulating the size of organizing centers.

Key words: Barhl, Apoptosis, Shh, Organizer, Diencephalon

Introduction

The neuroectoderm emerges from the dorsal ectoderm during gastrulation. Experiments performed mainly in amphibian embryos have established crucial roles for several secreted signaling proteins, including bone morphogenic proteins (BMPs), fibroblast growth factors (FGFs), Hedgehogs (HHs) and Wnt proteins, in neural induction and the establishment of the future dorsoventral (DV) and anteroposterior (AP) axes of the developing nervous system (reviewed by Gamse and Sive, 2000; Kiecker and Niehrs, 2001; Schier and Sive, 2001; Stern, 2002). Small groups of specialized cells serve as local sources of secreted factors and thereby act as 'organizing centers', patterning the neural tube by establishing the regional identity of adjacent domains.

Early in *Xenopus* development, the major source of secreted signaling proteins is the Spemann's organizer that give rise to the notochord underlying the neural plate and tube (reviewed by Joubin and Stern, 2001; Niehrs, 2004). The Spemann's organizer secretes the BMPs inhibitors Chordin, Noggin and Follistatin, which are involved in the decision of ectodermal cells to become epidermal or neural cells (Munoz-Sanjuan and Brivanlou, 2002; Stern, 2002; Wilson and Edlund, 2001), and Sonic Hedgehog (Shh), which is initially produced by the notochord and then later by the overlying neural floor plate. Both BMPs and Shh act as concentration-dependent morphogen, and specify the cell types produced in the neural tube (Barth et al., 1999; Dale and Jones, 1999; Lee et al., 2000). Shh also acts as a survival factor and as a mitogen, by driving the extensive expansion of the early brain (Britto et al., 2002; Dahmane et al., 2001; Lee et al., 2000; Thibert et al., 2003; Wallace, 1999). In these ways, BMPs and Shh help to regionalize the DV axis of the developing nervous system (Jacob et al., 2003; Ruiz i Altaba et al., 2003).

The position, size and shape of an organizing center has a major influence on the position, size and shape of the compartment that it patterns (Agarwala et al., 2001). It is less clear, however, how the size of organizing centers themselves is determined. Apoptosis plays a major role in controlling cell number during development (Jacobson et al., 1997). In *Xenopus* embryos, apoptosis occurs in a reproducible pattern in the neuroectoderm and the mesoderm, starting at the onset of gastrulation (Hensey and Gautier, 1998; Yeo and Gautier, 2003). BMP and Shh, have both been reported to have apoptosis-inducing and apoptosis-inhibiting properties, raising the possibility that morphogens may regulate apoptosis to help control the size of the organizing centers (Charrier et al., 2001; Golden et al., 1999; Litingtung and Chiang, 2000; Mabie et al., 1999).

Among the important target genes regulated by morphogens are homeobox genes. These genes encode gene regulatory proteins and specify regional identity by regulating 'effector' genes, which influence cell proliferation, adhesion, shape, migration, differentiation and survival (Puelles and Rubenstein, 2003; Rubenstein et al., 1998). Two *Drosophila*

homeobox genes *deformed* (*Dfd*) and *abdominal-B* (*Abd-B*), contribute to the maintenance of intersegmental boundaries through the regional activation of apoptosis (Lohmann et al., 2002). However, it is not known if Hox proteins directly regulate apoptosis during vertebrate development.

This study describes a novel function for *Barhl2* gene, a vertebrate homologue of *Drosophila barH* genes. In fly, the *barH* genes are expressed in the developing nervous system, act as pre-patterning genes and are involved in preventing ectopic retinal neurogenesis (Higashijima et al., 1992; Kojima et al., 2000; Lim and Choi, 2003; Sato et al., 1999). Vertebrate homologs of the *barH* genes have been isolated and their function examined during retina and ear development (Li et al., 2002; Mo et al., 2004; Poggi et al., 2004). In the vertebrate eye, Barhl2 function appears highly variable depending on the species. In the mouse retina it helps specify glycinergic amacrine cells from retinal progenitors (Mo et al., 2004); and in the *Xenopus* retina, it promotes ganglion cell fate, downstream of the atonal genes *Xath3* and *Xath5* (Poggi et al., 2004). We have isolated the *Xenopus* and mouse *Barhl2* genes, and studied their functions in *Xenopus* neurodevelopment. *Barhl2* loss-of-function and gain-of-function mutations produce defects in the establishment of the neural plate. Our data suggest that *Barhl2* normally regulates a cell survival pathway in the neural plate and dorsal mesoderm. *Barhl2* overexpression induces apoptosis in these tissues by a mechanism dependent on transcription, which differs from an unspecific cellular stress response. Specific inhibition of *Barhl2* expression by morpholinos leads to a decrease in apoptosis and an increase in the number of *chordin*- and *Xshh*-expressing cells. Finally Barhl2-defective embryos and embryos overexpressing the anti-apoptotic human *BCL2* gene have a similar phenotype. We propose that Barhl2-dependent apoptosis is necessary for correct formation of the axial organizing center of the *Xenopus* neural plate.

Materials and methods

Isolation of Barhl genes and construction of plasmids

A *Xenopus* stage 30 head and an E8.5 mouse embryo cDNA libraries were screened by PCR using degenerate primers (TAFSDHQ and KWKRQT). Fragments containing the Bar-homeobox encoding sequence were used to screen for cDNA clones. Mouse *Barhl2* and *Xbarhl2* coding sequences (from ATG to TGA) were subcloned in the pCS2 vector (Turner and Weintraub, 1994). A construct encoding the mouse protein, without the first 134 amino acids, was generated by PCR and subcloned into pCS2 to produce Barhl2ΔFIL. *Barhl2ΔFIL* was fused at its C-terminal end with amino acids 1 to 298 of the *Drosophila* Engrailed protein (Jaynes and O'Farrell, 1991), and subcloned into pCS2. *Xbarhl2*-coding sequences, without the stop codon, were amplified by PCR and subcloned in pCS2-Myc (Turner and Weintraub, 1994).

Embryos and injection

Xenopus embryos were obtained by in vitro fertilization, injected with synthetic RNA or morpholino and staged according to Nieuwkoop and Faber (Nieuwkoop and Faber, 1967). Capped RNAs were prepared from pCS2-derivatives (Ambion) and *Bcl2*-β RNA from pRC/CMV (Invitrogen). Antisense oligonucleotides coupled to the fluorescein were made by Gene Tools (Fig. 2C) and diluted into RNAse-free water. For *Xbarhl2ASI*, we used 10 ng for all experiments. For *Xbarhl2ASII*, 50 ng was generally used.

Reverse-transcription PCR

RNA from embryos was extracted using the Qiagen RNeasy Kit. RT-PCR analysis was carried out using the Superscript one-step Kit (Invitrogen). Sterile water was used as a control. Specific primers were used: *Xbarhl2*, 5′GCTCAACCAGCTGGAGAGGAGCTTTGA-GCG3′ and 5′TGTAGTTGTGGGTGGGGGGCAGGGGGAGTCC3′; *XEF-1α*, 5′CAGATTGGTGCTGGATATGC-3′ and 5′ACTGC-CTTGATGACTCCTAG3′; Chordin, 5′GTGGATTATGGCTGTG-GATTGCTCTCGC3′ and 5′AGCGACATCATCAGAACTCAGATA-AGG3′. Ncam 5′GTTGTAGCTAACCAAGCAGGACCACTG3′ and 5′GCAGTGGAAGAAACCAGCTCAGAAGC3′

Whole-mount in situ hybridization

In situ hybridization was performed using digoxigenin (DIG)-labeled probes, as described previously (Harland, 1991), with modifications (Turner and Weintraub, 1994). Antisense probes were generated for *Xbarhl2*, *Xshh*, *Xsox3*, *XK81*, *Xvent2*, *chordin*, *gli1* and *gli3* according to the manufacturer's instructions (Roche). Specimens were sectioned and embedded in agarose or Tissu-Tek. Frozen sections (10 μm) were cut on a Leica 2800 Frigocut-E cryostat at –24°C, thicker sections (50 μm) were cut on a Leica VT1000E vibratome.

Immunostaining

Immunostaining was performed using either a mouse monoclonal anti-Myc Cy3-conjugated antibody (Sigma) or a rabbit anti-phospho-histone H3 antibodies (Euromedex), as described previously (Saka and Smith, 2001). The anti-phospho-histone H3 antibody was detected using anti-rabbit (Ig) antibodies conjugated to alkaline phosphatase (Roche), followed by a staining using BCIP (5-bromo-4-chloro-3-indoyl-phosphate) as a substrate.

Protein isolation and western analysis

Total protein from embryos was extracted by shearing through a 22G needle in lysis buffer (Triton X-100 1%, 5 mM EDTA, 5 mM EGTA, 50 mM Tris, pH 8.0, 0.3 M NaCl and proteases inhibitors from Roche). Samples (3 and 10 μg) were processed for western analysis, using antibodies against Myc (Roche, #1667149) or activated Caspase 3 (Cell Signalling Technology, #9661).

Hydroxyurea (HU) treatment

Embryos were allowed to developed to stage 9.5 and grown until fixation in a solution of 30 mM hydroxyurea (Sigma) in 0.1×MMR, as described previously (Harris and Hartenstein, 1991; Saka and Smith, 2001).

TUNEL staining

Whole-mount TUNEL staining was performed as previously described (Hensey and Gautier, 1998; Yeo and Gautier, 2003). Early apoptosis is independent of cell proliferation (Yeo and Gautier, 2003); however, blocking cell division by incubation in HU appears to increase the number of embryos exhibiting a specific spatiotemporal pattern of cell death (our data) (Yeo and Gautier, 2003). The TUNEL analysis shown in Fig. 4A was performed on wild-type and *Xbarhl2AS*-injected embryos grown in HU from stage 9.5 onwards.

Cell death detection by ELISA

Cytoplasmic nucleosomal DNA was detected using a cell death detection ELISA kit (Roche). Five embryos were isolated for each time point and lysed in 50 μl incubation buffer. Lysates (10 μl) were incubated in 190 μl incubation buffer for 30 minutes on ice. The extracts were centrifuged for 10 minutes at 4°C. An aliquot (160 μl) of the supernatant was carefully removed, and ELISA was performed accordingly to the manufacturer's instructions.

Microdissection and transplantation

Neurula stage embryos were devitellinized and embedded in a clay-covered dish in 0.5×MMR. The tip of a 25G needle was used to cut

out different parts of the embryo at the indicated stage. The explant was peeled off, separated from the embryo and either RNA was extracted or the explant was inserted into a longitudinal incision made along the presumptive neural plate midline of the host embryo, down to the blastocoel and held in place for 30 minutes using a curved glass bridge.

X-gal staining

Embryos were fixed in MEMFA for 30 minutes, washed in phosphate buffer and transferred into X-gal staining solution (Coffman et al., 1990).

Results

Barhl2 cDNAs are highly conserved between metazoan species and *XBarhl2* is expressed from stage 10.5 onwards in *Xenopus* embryo

We isolated two complete cDNAs that contained a single open reading frame encoding proteins of, respectively, 327 (XBarhl2) and 384 amino acids (mouse Barhl2). Phylogenetic analysis shows that Barhl2 proteins are more closely related to *Drosophila* BarH, nematode CEH-30 and CEH-31, and vertebrate Barhl1 proteins than to mammalian Barx proteins (Fig. 1A).

We examined the expression pattern of *Xbarhl2* during early *Xenopus* embryogenesis. By RT-PCR analysis we detected *Xbarhl2* transcripts from stage 10.5 onwards in the dorsal part of the embryo (Fig. 1B, parts a,b). Whole-mount in situ analysis at stage 14 confirmed the described presence of *Xbarhl2* transcripts in a region fated to become the dorsal diencephalon (Fig. 1C) (Patterson et al., 2000). It also suggested its presence along the midline (Fig. 1D), confirmed by RT-PCR analysis on the posterior neural plate and posterior dorsal mesoderm, as on the midline of stage 14 embryos (Fig. 1E, parts a,b). We focused our study on deciphering the role of *Xbarhl2* in these tissues between stage 10.5 and stage 18.

Manipulation of the level of *XBarhl2* expression interferes with neural plate formation

The N-terminal region of the Barhl2 protein contains two conserved domains, FIL1 and FIL2, that are composed mainly of phenylalanine, isoleucine and leucine (Saito et al., 1998). A sequence comparison between the FIL domains and the Eh1 repression domain present in the Engrailed protein established that these domains are similar (Fig. 2A). Eh1 domains are present in Engrailed, Goosecoid, Nkx1 and Msh classes of homeoproteins, and have been shown to repress transcription in vivo and in vitro (Smith and Jaynes, 1996). We removed the *eh1* domains from the mouse *Barhl2* cDNA, generating *Barhl2ΔFIL* (Fig. 2B). We fused the repressor domain of the *Drosophila* Engrailed protein to *Barhl2ΔFIL* (*Barhl2ΔFIL-enR*, Fig. 2B). We used two different *Xbarhl2* antisense morpholinos (*Xbarhl2ASI* and *Xbarhl2ASII*) to inhibit *Xbarhl2* activity, together with a control morpholino (*Xbarhl2ASIII*). These oligonucleotides were designed in a region overlapping the translational initiation site, so that they do not bind to mouse *Barhl2* or *Xbarhl1* mRNA (Fig. 2C). We used *Xsox3* as an early marker of neural induction (Penzel et al., 1997) and epidermal keratin 81 (*XK81*) (Jamrich et al., 1987) as an epidermal marker. For all constructs we injected the specified RNA together with GFP RNA used as a tracer.

We injected *Xbarhl2* or mouse *Barhl2* RNA or antisense morpholinos into one dorsal blastomere of four-cell embryos. Results were similar with mouse *Barhl2* and *Xbarhl2*, and we

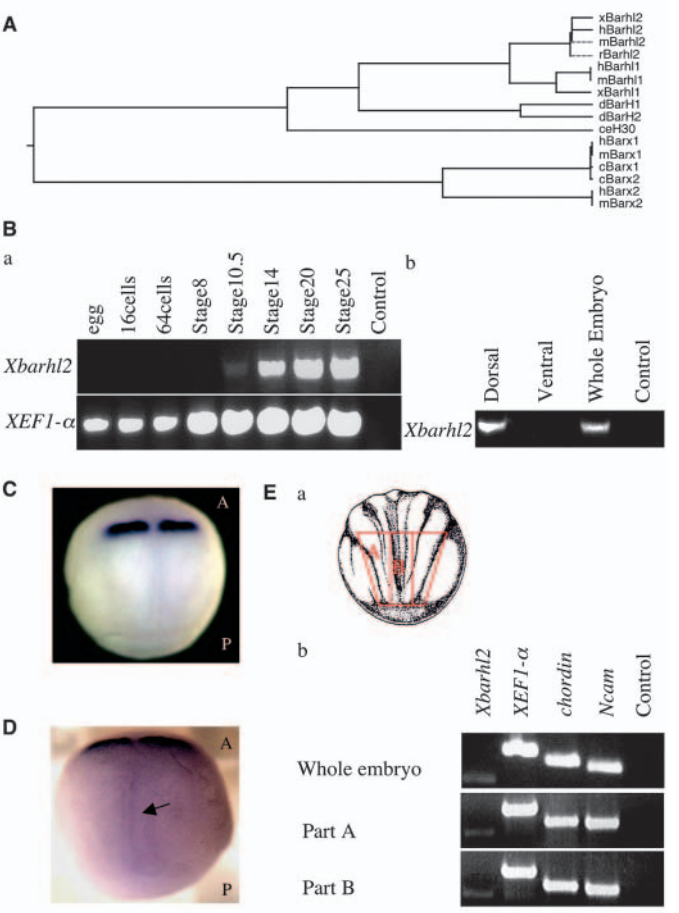

Fig. 1. Phylogenetic analysis and early expression pattern of XBarhl2. (A) Phylogenetic tree based on identity in 60 amino acid homeobox region between the Barhl proteins in human, mouse, rat, *Xenopus*, *C. elegans* and *Drosophila* and the Barx proteins of human and chicken (Barlow and Francis-West, 1997; Edelman et al., 2000; Hjalt and Murray, 1999). Mouse Barhl2 (Mo et al., 2004), mouse Barhl1 (Bulfone et al., 2000; Li et al., 2002) and XBarhl2 (Patterson et al., 2000; Poggi et al., 2004) sequences were determined by us. Human Barhl2 (GenBank AL355867) and human Barhl1 (GenBank AL354735) sequences were predicted from their genomic DNA sequences; rat Barhl2 (MBH1) (Saba et al., 2003; Saito et al., 1998). The tree was determined using MegAlign from the Lasergene Navigator, licensed by DNAStar. d, *Drosophila melanogaster*; m, *Mus musculus*; r, *Rattus norvegicus*; x, *Xenopus laevis*; d-rer, *Dario rerio*; ce, *Caenorhabditis elegans*; h, *Homo sapiens*. (B) Expression of *Xbarhl2* as determined by RT-PCR analysis on embryos at different embryonic stages and dissected parts of embryos. (a) *Xbarhl2* starts to be expressed at stage 10.5. *XEF-1α* was analyzed as a control. (b) At stage 10.5 *Xbarhl2* is expressed in the dorsal part of the embryo. (C,D) Whole-mount in situ hybridization of embryos, using *Xbarhl2* as a probe. (C) Dorsal view of stage 14 embryos showing expression of *Xbarhl2* in the dorsal diencephalon. (D) Same embryo as C rotated showing expression along the midline (arrow). A, anterior; P, posterior. (E) RT-PCR analysis. (a) Drawing of a stage 14 embryo showing dissected parts (Nieuwkoop and Faber, 1967). (b) *Xbarhl2* is expressed in the posterior neural plate, posterior dorsal mesoderm and in the midline of stage 14 embryo. *Chordin* and *Ncam* were analyzed as mesodermal and neuroectodermal markers, respectively.

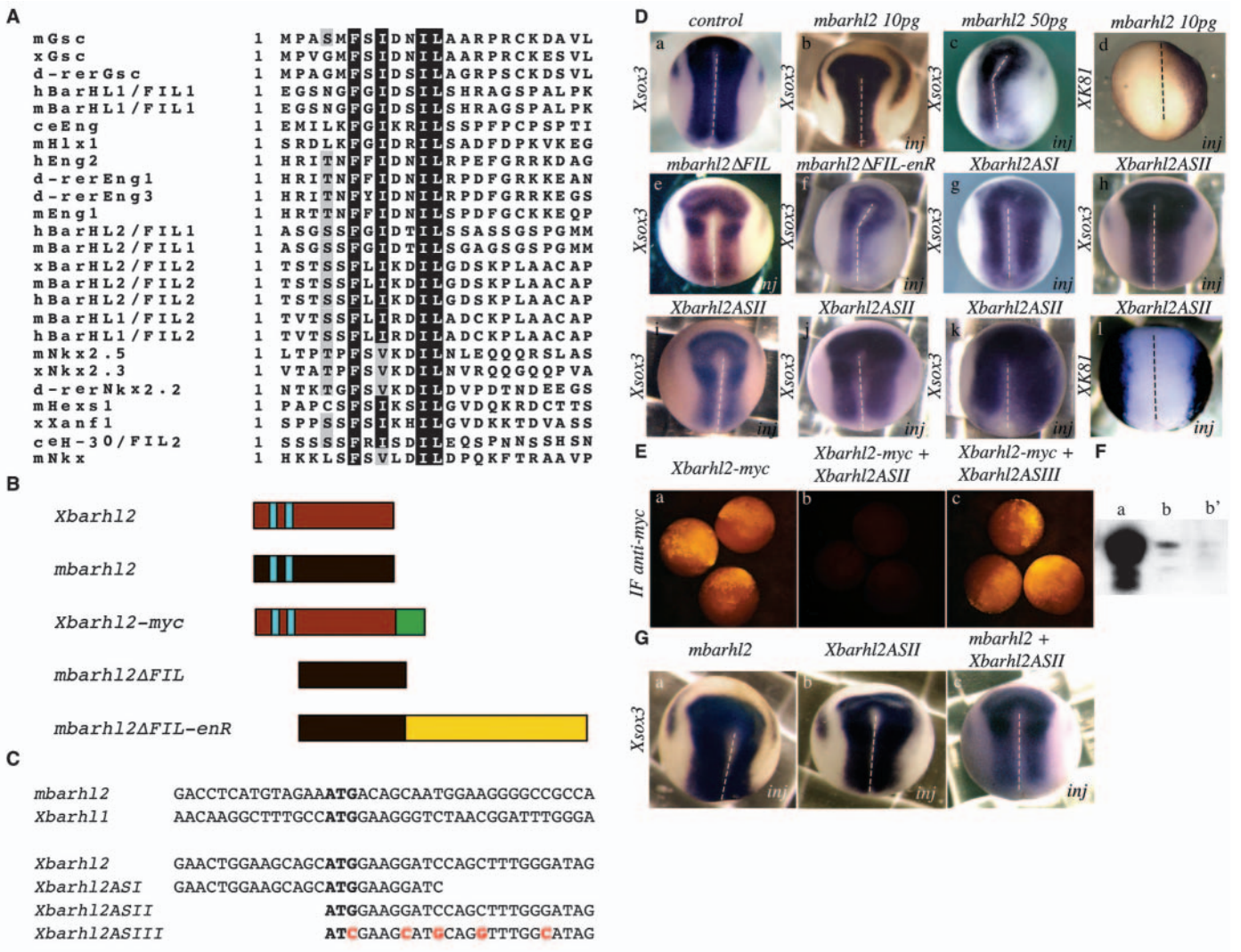

Fig. 2. Changes in *Barhl2* levels alter neural plate formation. (A) Sequence comparison between the Eh1 motifs of Gsc, Eng, Nkx, Anf-1, Hesx1 and Msx, and the FILs domains of Barhl proteins. Black shading indicates identical residues, gray shading indicates similarity. Most of the sequences, except for *Barhl* members, come from Smith and Jaynes (Smith and Jaynes, 1996). (B) Map of the RNA constructs. The two blue boxes indicate the FIL domains; the green box indicates the Myc epitope; the yellow box indicates the Engrailed repression domain. (C) Sequences of the *Xbarhl2* antisense morpholinos. The five mispairs in *Xbarhl2ASIII* are in red and the ATG is in bold. For comparison, the N-terminal sequences of mouse *Barhl2*, *Xbarhl1* and *Xbarhl2* are shown. (D) In situ hybridization of embryos injected with mouse *Barhl2*, *Barhl2ΔFIL*, *Barhl2ΔFIL-enR*, *Xbarhl2ASI*, *Xbarhl2ASII*, *Xbarhl2ASIII* and analyzed at stage 15. Dorsal view, anterior end upwards. The broken line indicates the midline and 'inj' indicates the injected side. Embryos labeled with *Xsox3* as probe: (a) control; injected with mouse *Barhl2* at (b) 10 pg and (c) 50 pg; (e) injected with mouse *Barhl2ΔFIL* (100 pg); (f) injected with mouse *Barhl2ΔFIL-enR* (50 pg); (g) injected with *Xbarhl2ASI*; (h) injected with *Xbarhl2ASII*; injected with *Xbarhl2ASII* at (i) 20 ng, (j) 50 ng and (k) 100 ng. Embryos labeled with *XK81* as a probe: injected with mouse *Barhl2* at 10 pg (d); injected with *Xbarhl2ASII* (l). (E) Two-cell embryos were injected in one blastomere and analyzed at stage 9. Representative embryos are shown under fluorescent light. (a) Embryos injected with *Xbarhl2-myc* (100 pg); (b) injected with *Xbarhl2-myc* (100 pg) together with *Xbarhl2ASII* (100 ng); (c) injected with *Xbarhl2-myc* (100 pg) together with *Xbarhl2ASIII* (100 ng). (F) Western analysis on protein extracts from stage 9 embryos injected with *Xbarhl2-myc* (100 pg) together with: *Xbarhl2ASIII* (100 ng) (a); *Xbarhl2ASII* (50 ng) (b) or *Xbarhl2ASII* (100 ng) (b′) using anti-Myc antibody. (G) Embryos labeled with *Xsox3* as probe. The percentage of embryos exhibiting the staining patterns: (a) injected with mouse *Barhl2* (10 pg), 78%; (b) injected with *Xbarhl2ASII* (50 ng), 88%; (c) injected with mouse *Barhl2* (10 pg) together with *Xbarhl2ASII* (50 ng), 60%.

mostly used mouse *Barhl2* for further experiments. At stage 14, we observed a dose-dependent decrease in the width of the *Xsox3* expression domain on embryos injected with mouse *Barhl2* (Fig. 2D, part b). Injection of over 50 pg of mouse *Barhl2* caused the *Xsox3* expression domain to partially disappear (Fig. 2D, part c). The effects on *XK81* expression were complementary to those seen with *Xsox3* (Fig. 2D, part d). Injection of *Barhl2ΔFIL* produced embryos similar to control siblings (Fig. 2D, part e), when injection of *Barhl2ΔFIL-enR* produced a phenotype similar to that produced by injections of mouse *Barhl2* (Fig. 2D, part f), indicating that Barhl2 functions as a repressor at these stages. In contrast to the effect produced by mouse *Barhl2*, the neural plate of *Xbarhl2ASI*- or *Xbarhl2ASII*-treated embryos was

larger on the injected side than on the control side (Fig. 2D, parts g,h). This effect was observed along the entire AP axis at all stages analyzed. The expansion of the neural plate was dose dependent, as shown by injection of 20 ng (no effect, Fig. 2D, part i), 50 ng (a 30% increase in size, Fig. 2D, part j) and 100 ng (50%, Fig. 2D, part k) of *Xbarhl2ASII*. Conversely, the extent of the epidermal territory was decreased in *Xbarhl2ASI* or *Xbarhl2ASII*-treated embryos (Fig. 2D, part l). We did not detect any changes in expression pattern of either *Xsox3* or *XK81* upon injection of *Xbarhl2ASIII* (data not shown, n=60).

To establish the specificity of the morpholino effect, we tested the ability of *Xbarhl2ASII* to inhibit translation of the *Xbarhl2* mRNA. Myc-tagged *Xbarhl2* (*Xbarhl2-myc*, Fig. 2B) was co-injected with *Xbarhl2ASII* or *Xbarhl2ASIII* as a control. Immunostaining of the embryos revealed that *Xbarhl2ASII* inhibited the translation of *Xbarhl2-myc* mRNA (Fig. 2E, part b), while *Xbarhl2ASIII* did not (Fig. 2E, part c). A specific dose-dependent inhibition of *Xbarhl2-myc* messenger translation by the *Xbarhl2ASII* in embryos was confirmed by western blot analysis on extracts from embryos injected with increasing doses of *Xbarhl2ASII* (Fig. 2F).

We tested *Xbarhl2ASII* as a specific inhibitor of endogenous XBarhl2 activity by co-injecting 10 pg mouse *Barhl2* (Fig. 2G, part a) with 50 ng (Fig. 2G, part b) of *Xbarhl2ASII*. When *Xsox3* was used to assess neural plate development, we observed that *Xbarhl2ASII* rescued the phenotype induced by mouse *Barhl2* overexpression in 60% of the embryos (Fig. 2G, part c). These data provide strong evidence that the *Xbarhl2ASII* were acting by specifically inhibiting endogenous XBarhl2 activity in our injection experiments. As the effects of *Xbarhl2ASI* and *Xbarhl2ASII* were similar, we refer to it as *Xbarhl2AS*.

Thus, increasing Barhl2 activity reduces the neural plate territory, whereas reducing Barhl2 activity increases it. The effect of Barhl2 depends on its two Eh1 domains, and is likely to involve Barhl2-mediated transcriptional repression.

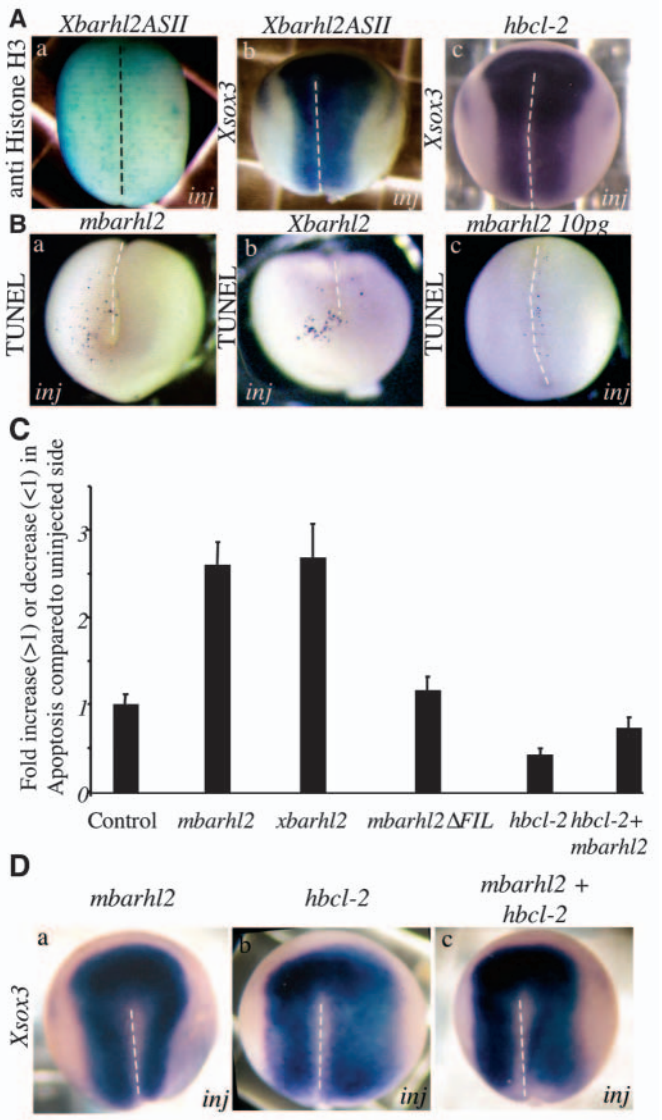

Fig. 3. Barhl2 induces apoptosis in *Xenopus* neuroectoderm. (A) Stage 15 embryos. (a) Embryo injected with *Xbarhl2AS* and immunostained using anti-phospho-histone H3 antibody. (b,c) In situ hybridization using *Xsox3* as a probe on embryos injected with: (b) *Xbarhl2AS* and treated with HU; (c) human *BCL2* (500 pg). (B) TUNEL staining of stage 15 embryos representative of those injected with mouse *Barhl2* (20 pg) (a), *Xbarhl2* (20 pg) (b) and mouse *Barhl2* (10 pg) (c). (a,b) Anterior views, dorsal upwards; (c) dorsal view, anterior upwards. (C) Number of TUNEL$^+$ cells were counted on the injected side and compared to the number on the control side at stage 15. The results were assessed by Student's *t*-test. Results are shown as mean±s.e.m. Injection of mouse *Barhl2* increased apoptosis 2.6 times (10 pg to 25 pg) (n=70, P=3.10^{-8}), as does *Xbarhl2* (20 pg, n=20, P=9.10^{-5}). Injection of human *BCL2* (500 pg) reduced apoptosis (n=35, P=0.002), and the effect of *Barhl2* (10 pg) was reversed by co-injection of human *BCL2* (500 pg) (n=40, P>0.01). Injection of mouse *Barhl2ΔFIL* had no effect (n=28, P>0.01). (D) In situ hybridization using *Xsox3* as a probe of stage 14 embryos injected with: (a) mouse *Barhl2* (10 pg), 82%; (b) human *BCL2* (500 pg) 89%; and (c) mouse *Barhl2* (10 pg) and human *BCL2* (500 pg), 60%.

Barhl2 induces apoptosis in neuroectodermal cells of the neural plate

In principle, Barhl2 overexpression may decrease neural plate formation by inhibiting neural induction, inhibiting neuroectodermal cell proliferation or increasing neuroectodermal cell death or by some combination of these.

The neuroectodermal expression pattern of *Barhl2* argues against a role for Barhl2 as a direct inhibitor of neural induction. We assessed whether Barhl2 regulates neuroectodermal cell proliferation. Embryos injected with *Xbarhl2AS* were immunostained using an antibody against phosphorylated histone H3, which specifically recognizes mitotic chromosomes (Saka and Smith, 2001). We did not observe a significant change in the number of mitotic cells on the *Xbarhl2AS*-injected side compared with the control side (Fig. 3A, part a). When similarly injected embryos were allowed to develop from the gastrula stage onwards in hydroxyurea (HU), which effectively blocks DNA replication and cell division (Newport and Dasso, 1989), *Xbarhl2AS*-injected side exhibited a typical increase in the *Xsox3* expression domain compared with the control size (Fig. 3A, part b). These observations argue against a role for Barhl2 as a modulator of cell proliferation at these early stages.

Therefore we tested whether the overexpression of *Barhl2* decreased neural plate formation by increasing apoptosis in neuroectodermal cells. Apoptosis can be inhibited by

overexpression of the human *BCL2* gene, which encodes the apoptosis inhibitor BCL2 (Yeo and Gautier, 2003). We injected *BCL2* and followed the establishment of neural and epidermal territories using *Xsox3* and *XK81*. As we had observed with injections of *Xbarhl2AS*, we saw an increase in the size of the neural plate and a decrease in the size of epidermis on the *BCL2* injected side along the entire AP axis of the embryos (Fig. 3A, part c, data not shown) (Yeo and Gautier, 2003), consistent with the possibility that *Xbarhl2AS* increases neural plate development by decreasing apoptosis there.

We injected different quantities of mouse *Barhl2*, *Xbarhl2* or, as a control, RNA encoding GFP or XPax6, and followed apoptosis by TUNEL analysis in *Xenopus* neuroectoderm (Fig. 3B,C). We observed a reproducible increase of 2.6 in the number of TUNEL-positive nuclei on the injected side of stage 15 embryos treated with mouse *Barhl2* or *Xbarhl2* compared with the control side (Fig. 3B,C). No difference was detected when RNA encoding GFP or XPax6 was injected as a control (data not shown), or with ventral injections of mouse *Barhl2* (n=53, data not shown). Interestingly, we observed a specific pattern of apoptotic nuclei in embryos injected with the lowest dose of mouse *Barhl2*: over 50% of the TUNEL-positive cells were located within a narrow stripe bordering the midline of the posterior neural plate (Fig. 3B, part c), suggesting that these cells were most sensitive to the apoptosis-promoting effect of Barhl2. We did not detect any increase in the frequency of apoptotic cells in embryos dorsally injected with *Barhl2ΔFIL* (Fig. 3C), showing that *Barhl2* transcriptional activity is strictly necessary for the pro-apoptotic effect of Barhl2. Finally we co-injected mouse *Barhl2* and *BCL2*, and studied these embryos by TUNEL analysis. As shown in Fig. 3C, there was no significant difference between the number of apoptotic nuclei in embryos injected with both mouse *Barhl2* and *BCL2*, when compared with the controls, confirming that *Barhl2* overexpression promotes apoptosis.

To see if the pro-apoptotic effect of *Barhl2* correlated with the observed phenotype of *Barhl2*-overexpressing embryos, we studied the expression of *Xsox3* in embryos injected with mouse *Barhl2*, *BCL2* or mouse *Barhl2* together with *BCL2* at the same doses as those used for TUNEL analysis. We observed that *hbcl2* expression rescued the *Barhl2*-induced phenotype in over 60% of the embryos at this stage (Fig. 3D).

Thus, Barhl2 can induce apoptosis in dorsal cells through its transcriptional regulatory function. Cells localized along the midline appear to be most sensitive to the pro-apoptotic activity of Barhl2, and the reduction in neural plate territory caused by *Barhl2* overexpression can be rescued by overexpression of the apoptotic inhibitor Bcl2.

Inhibition of endogenous Barhl2 activity partially inhibits endogenous apoptosis

To assess the normal function of Barhl2 pro-apoptotic activity we first used the TUNEL assay to follow endogenous apoptosis from stage 12 to stage 18. At stage 12, apoptotic nuclei were mainly detected around the blastopore and along the axial midline as it forms (Fig. 4A, part a) (Hensey and Gautier, 1998; Yeo and Gautier, 2003). At stage 15, the apoptotic cells were detected in two stripes along the midline (Fig. 4A, part b). At stage 18, we observed apoptotic cells in the neural grove and in the anterior part of the neural plate (Fig. 4A, parts c,d). As described by others, we observed an asymmetric pattern of

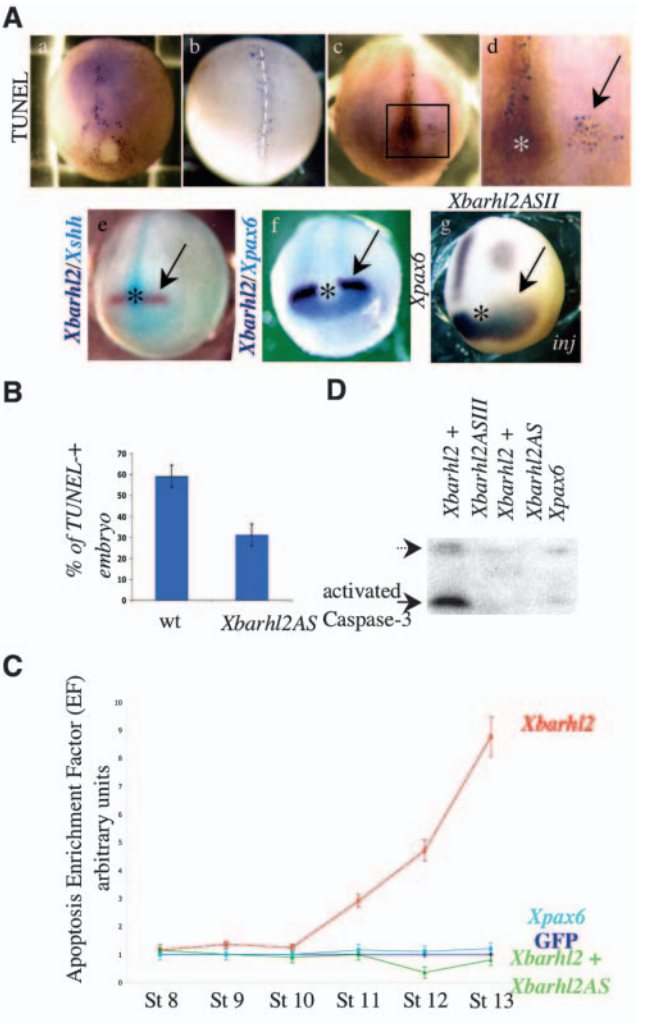

Fig. 4. Barhl2 pro-apoptotic activity is normally involved in regulating endogenous apoptosis. (A) TUNEL staining of stage 12.5 (a), stage 15 (b) and stage 18 (c,d) embryos. (d) Magnified view of the boxed region in c. (e,f) Double in situ hybridization of stage 18 embryos using digoxigenin- and fluorescein-labeled RNA probes: *Xbarhl2* (dark blue) and *Xshh* (light blue) (e); *Xbarhl2* (dark blue) and *Xpax6* (light blue) (f). (g) In situ hybridization of *Xbarhl2AS*-injected embryo using *Xpax6* as a probe. (a,b) Dorsal views, anterior upwards. (c-f) Anterior views, dorsal upwards. (B) Comparison of the percentage of TUNEL-positive embryos (defined as exhibiting more then 30 apoptotic nuclei in the axial midline, i.e. where endogenous apoptosis normally occurs) between wild-type embryos and embryos injected in the two dorsal blastomeres at the two-cell stage with *Xbarhl2AS*. Each experimental batch (n=60) was assessed independently. Three different experiments were performed and the results are shown as mean±s.e.m. (C) Kinetics of *Xbarhl2* induced apoptosis between stage 8 and stage 13. Embryos were injected in one dorsal blastomere at the two-cell stage with *GFP* (dark blue), *Xbarhl2* (red), *Xbarhl2* together with *Xbarhl2AS* (green) or *Xpax6* (light blue) and collected at indicated developmental stages. Cell death was measured by cell death detection ELISA. The apoptotic EF is calculated using *GFP*-injected embryos as a control. We carried out three different experiments and the results are shown as mean±s.e.m. (D) Western blot analysis on 3 μg of protein extracted from stage 12 embryos injected with *Xbarhl2* (100 pg) together with *Xbarhl2ASIII* or *Xbarhl2* (100 pg) together with *Xbarhl2ASII*, *Xpax6* (100 pg), as indicated. The arrow indicates the large (19 kDa) cleaved caspase 3 fragment. The broken arrow shows a nonspecific band used as an internal control.

apoptotic cells between the right and left sides of the embryo. Double in situ hybridization analysis with *Xshh* (Fig. 4A, part e), which is expressed in midline structures and the prechordal plate (Ekker et al., 1995), and *Xpax6* (Fig. 4A, part f), which is expressed in the forebrain (Hirsch and Harris, 1997), suggested that this anterior neural plate area containing apoptotic cells could correspond to the domain of *Xbarhl2* expression. In agreement with this hypothesis, we observed a dramatic expansion of the *Xpax6* expression domain, most strikingly in the dorsal diencephalic area where its expression overlaps with that of *Xbarhl2*, in embryos injected with *Xbarhl2AS* (Fig. 4A, part g). These data are consistent with the possibility that Barhl2 can promote apoptosis at these early developmental stages.

We examined whether inhibition of Barhl2 activity could change the level of endogenous apoptosis. Using the TUNEL assay, we compared apoptosis in stage 15 wild-type embryos and embryos injected with *Xbarhl2AS*. When Barhl2 activity was inhibited in this way, we observed a reproducible decrease in the number of apoptotic cells per embryo (Fig. 4B), strengthening the hypothesis that Barhl2 normally acts on a cell survival pathway.

The zygotic apoptotic program in the *Xenopus* embryo comes into play at the onset of gastrulation, when *Xbarhl2* transcripts are first detected. We assessed whether Barhl2 pro-apoptotic activity was dependent on the endogenous apoptotic program. Embryos were injected with *Xbarhl2*, *GFP* or *Xbarhl2*, together with *Xbarhl2AS*. Apoptosis was measured in extracts from stage 8 to stage 13 embryo using an ELISA assay for cytoplasmic histone-associated mono- and oligo-nucleosomes that are specifically released during the apoptotic process (Veenstra et al., 1998). As shown in Fig. 4C, we observed, from stage 10.5 onwards, a steady increase in the apoptotic enrichment factor (EF) that is the number of dying/dead cells in a specimen over the number of dying/dead cells in the control GFP-injected embryos (Fig. 4C, EF=9 at stage 13). Co-injection of *Xbarhl2AS* with *Xbarhl2* completely inhibited apoptosis. The measured EF in embryos injected with *Xbarhl2* and *Xbarhl2AS* was less then one (Fig. 4C, EF=0.8 at stage13), in agreement with our observation that *Xbarhl2AS* can partly inhibit endogenous apoptosis.

Cellular stress, including that caused by the overexpression of transcription factors, can trigger apoptosis in an unspecific way (Kumar and Cakouros, 2004). As a control, we measured the apoptotic EF in embryos injected with *Xpax6*. We observed only a slight increase in the apoptotic EF in the *Xpax6*-injected embryos (Fig. 4C, EF=1.2 at stage 13). We conclude that the apoptotic response of cells upon *Barhl2* overexpression is not due to an unspecific stress response.

We followed the presence of activated Caspase 3, the

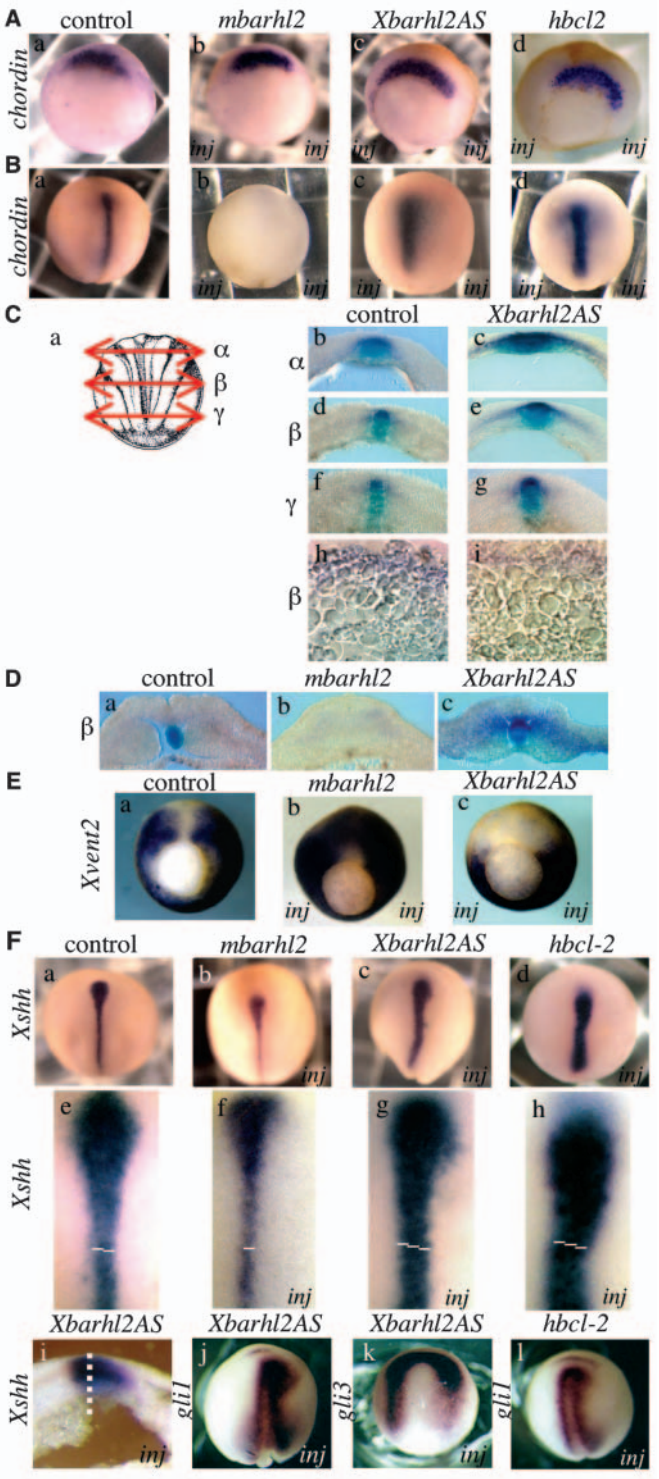

Fig. 5. Manipulation of Barhl2 levels changes the number of *chordin*- and *Xshh*-expressing cells. In situ hybridization of embryos injected in either two (A-E) or one (F) dorsal blastomere with mouse *Barhl2*, *Xbarhl2AS* or human *BCL2*. Embryos are shown at (A) stage 10, (B,C) stage 15, (D) stage 18, (E) stage 12, (F) stage 15. (A-D) In situ hybridization using *chordin* as a probe. (A,B) control (a), mouse *Barhl2* (b), *Xbarhl2AS* (c), human *BCL2* (d). (C) Serial sections. (a) Scheme of a stage 14 embryo showing position of cuts. (b-i) Sections of *Xbarhl2AS*-injected embryo. α level: (b) control; (c) *Xbarhl2AS*. β level: (d) control; (e) *Xbarhl2AS*. γ level: (f) control; (g) *Xbarhl2AS*. Thin β level sections in the prospective notochord area: (h) control; (i) *Xbarhl2AS*. (D) β level sections of stage 18 embryos: (a) control; (b) mouse *Barhl2*; (c) *Xbarhl2AS*. (E) In situ hybridization using *Xvent2* as a probe: (a) control; (b) mouse *Barhl2*; (c) *Xbarhl2AS*. (F) In situ hybridization using *Xshh* as a probe (a-i). (a) Control; (b) mouse *Barhl2*; (c) *Xbarhl2AS*; (d) human *BCL2*. (e-h) Magnified views of a-d, respectively. (g) β level section of *Xbarhl2AS*-injected embryo. (h,l) In situ hybridization using *gli1* as a probe. (i) In situ hybridization using *gli3* as a probe. The line in e-h is shown as a scale indicator.

trademark of an apoptotic process (Adams, 2003), in embryos injected with *Xbarhl2*, with *Xbarhl2* and *Xbarhl2AS*, or with *Xpax6*. We observed a specific induction of Caspase 3 cleavage in stage 12 embryos injected with *Xbarhl2*, which was totally inhibited in the presence of *Xbarhl2AS* (Fig. 4D).

We conclude that Barhl2 normally promotes apoptosis at the same time as the endogenous zygotic apoptotic program comes into play.

Embryos defective for Barhl2 activity exhibit an increase in the number of both *chordin*- and *Xshh*-expressing cells

Cell death occurs along the forming axial structures in neurulating *Xenopus* embryos (our data) (Yeo and Gautier, 2003). To assess which cells undergo *Barhl2*-mediated apoptosis, we followed the development of the prospective notochord and the floorplate territories in embryos in which *Barhl2* expression was experimentally modified.

We used *chordin* as a marker of axial mesoderm territory (Sasai et al., 1994). The pattern of *chordin* expression was normal at stage 10 in both mouse *Barhl2*- and *Xbarhl2AS*-injected embryos, showing that the Spemann's organizer developed normally (Fig. 5A). At stage 15, we observed the disappearance of *chordin*-expressing cells in mouse *Barhl2*-injected embryos (Fig. 5B, part b). Conversely, in *Xbarhl2AS*-injected embryos, the area of expression of *chordin* was broader (Fig. 5B, part c). To test if the increase in *chordin*-expressing area might be due to a decrease in the pro-apoptotic effect of Barhl2, we injected human *BCL2* instead of the morpholino. Similar to what we observed with *Xbarhl2AS*, we did not detect any defect in *chordin* expression at stage 10 (Fig. 5A, part d), but an increase in the area of *chordin* expression at stage 15 (Fig. 5B, part d).

A series of anterior-to-posterior transverse sections from stage 15 stage embryos injected with *Xbarhl2AS* confirmed an increase in the size of the *chordin*-expressing area that was greater at the anterior end of the embryos (Fig. 5C, parts a-g). Observations of serial frozen sections of control and *Xbarhl2AS*-injected embryos indicated that this increase is not due to a change in the size of *chordin*-expressing cells (Fig. 5C, parts h,i). We confirmed these results with transverse sections of similarly treated stage 18 embryos (Fig. 5D), and found that the axial territory failed to develop in *Barhl2*-overexpressing embryos (Fig. 5D, part b). Conversely, there was a surplus of *chordin*-expressing cells in embryos in which Barhl2 activity was inhibited (Fig. 5D, part c).

Chordin acts as a BMP inhibitor. An increase in the number of *chordin*-expressing cells should generate an overall decrease in BMP signaling. We followed changes in the expression pattern of *Xvent2* that is under the control of BMP signaling (Onichtchouk et al., 1996). As shown in Fig. 5E, in stage 12 mouse *Barhl2*-injected embryos *Xvent2* area of expression was shifted dorsally towards the midline compared with control embryos (Fig. 5E, part b). Whereas in stage 12 *Xbarhl2AS*-injected embryos, the *Xvent2* expression area was shifted ventrally (Fig. 5E, part c). We concluded that Barhl2 indirectly modulates BMP signaling.

We studied the expression of Shh that is expressed in the prospective notochord and in the floorplate (Fig. 5F). One side injection of mouse *Barhl2* caused a decrease of about 50% in the size of the floorplate (Fig. 5F, parts b,f), while a similar injection of *Xbarhl2AS* caused an increase in this territory (Fig. 5F, parts c,g). We confirmed the increase in the number of *Xshh*-expressing cells in the mesoderm and the neuroectoderm by examination of sections (Fig. 5F, part i). The Gli transcription factors mediate the effects of the Shh signaling. We followed the expression of *gli1*, which is a direct target of Shh signaling, and *gli3*, which is repressed by Shh. Embryos injected with *Xbarhl2AS* showed increased Shh activity in the posterior neural plate, as judged by an increase in the area of *gli1* expression on the injected side (Fig. 5F, part j) and a decrease in *gli3* expression (Fig. 5F, part k).

In embryos where apoptosis was inhibited by injecting *BCL2*, we observed a similar enlargement of the *Xshh* territory of expression (Fig. 5F, parts d,h), and an increase in Shh activity in the posterior neural plate, indicated by an increase in *gli1* expression (Fig. 5F, part l).

We conclude that endogenous Barhl2 normally plays an important role in limiting the number of cells expressing *chordin* and cells expressing *Xshh* and indirectly in regulating BMP and Shh signaling.

Barhl2 gain-of-function embryonic defects are partially rescued by notochord and floor-plate grafts

Our observations are consistent with the possibility that *Barhl2* overexpression decreases the number of notochord and floor-plate cells. The resulting decrease in their organizing activity could be partly responsible for the observed developmental defects. We assessed the ability of a grafted notochord and floor plate from wild-type embryos to rescue *Barhl2*-injected embryos. Embryos were injected with either β-galactosidase or mouse *Barhl2*, together with GFP as a tracer. Between stage 12 and stage 14, the prospective midline of wild-type donor embryos was grafted to mouse *Barhl2*-injected host embryos as shown in Fig. 6A. Embryos were allowed to develop until stage 40 and stained for β-galactosidase activity. Control embryos exhibited only slight developmental defects and had normal heads (Fig. 6B). Injections of mouse *Barhl2* inhibited the formation of dorsal structures, with the eye and cement gland failing to form in 90% of embryos (Fig. 6C). By contrast, over 50% of *Barhl2*-injected embryos with wild-type graft developed head structures (Fig. 6D). As shown by β-galactosidase staining, most of the rescued structures did not derived from the graft. These observations suggest that the phenotype of mouse *Barhl2*-overexpressing embryos is mainly due to decrease axial organizing activity during neurulation.

Discussion

The Barhl2 DNA binding homeodomain protein is normally part of a pathway regulating apoptosis in early *Xenopus* neurodevelopment

EPCD affects proliferating and early differentiating cells and mainly occurs during neurulation, neural crest formation and eye induction and formation (reviewed by de la Rosa and de Pablo, 2000; Kuan et al., 2000; Yeo and Gautier, 2004). Here, we provide evidence that the highly conserved *Barhl2* gene is part of a pathway that regulates EPCD. Overexpression of *Barhl2* through injection of RNA into the dorsal part of the embryo induces an increase in apoptosis that cannot be attributed to a nonspecific cellular stress response. Inhibition of Barhl2 activity diminishes endogenous apoptosis and

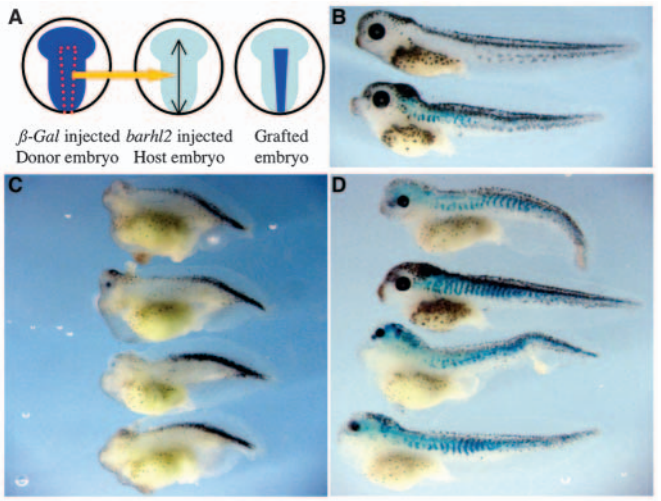

Fig. 6. A neurula stage graft of notochord and floorplate rescues *Barhl2* gain-of-function phenotype. (A) Notochord and floorplate explants from stage 12-14 β-galactosidase (100 pg)-injected donor embryos were grafted in the presumptive neural plate midline of wild-type or mouse *Barhl2* (25 pg)-injected embryos. (B-D) The embryos were analyzed at stage 40. β-Galactosidase activity is revealed in blue. (B) Control embryo (top) and control embryo grafted with wild-type explants (bottom). (C) Mouse *Barhl2*-injected embryos (n=40). (D) Mouse *Barhl2*-injected embryos grafted with explants from β-galactosidase-injected wild-type donors (n=41).

increases the number of both *chordin*- and *Xshh*-expressing cells in the prospective notochord and floorplate. We show that the pro-apoptotic activity of Barhl2 requires transcriptional activity, and that the Barhl2 protein acts as a transcriptional repressor at these stages of development, presumably through the recruitment of the co-repressor Groucho/TLE, which binds to the Eh1 motif (Muhr et al., 2001). These data are in agreement with our observations that cells localized along the midline appear to be more sensitive to the pro-apoptotic activity of Barhl2, and that this pro-apoptotic activity is activated at the same time as the endogenous zygotic apoptotic program comes into play.

Barhl2-regulated apoptosis plays a role in limiting the size of the forming axial neural organizer

As morphogenetic gradients of both BMP and Shh are essential for outgrowth and patterning of the neural plate, the number of cells producing these morphogens must be tightly regulated. Barhl2-regulated apoptosis appears as part of the system that controls both the size and correct establishment of the axial organizer during the rapid growth of the gastrulating embryo. A similar role for apoptosis has been described in vertebrate limb development. There a Shh-producing polarizing region acts as an organizing center and apoptosis regulates the number of Shh-expressing cells (Sanz-Ezquerro and Tickle, 2000). The location, size and shape of an organizing center determines the size, shape and orientation of the target tissue (Agarwala et al., 2001). *Xbarhl2AS*-injected embryos phenotype is similar to the phenotype seen in BMP4 loss-of-function (Dale and Jones, 1999; Gamse and Sive, 2000) and in Bcl2 gain-of-function (Yeo and Gautier, 2003) experiments. Conversely, *Barhl2* overexpression causes a ventralization phenotype similar to that seen in BMP4 gain-of-function experiments (Dale and Jones, 1999; Gamse and Sive, 2000). A neurula stage graft of notochord and floor-plate cells into an mouse *Barhl2* overexpressing embryo partially rescues the formation of head structures, strongly arguing that the Barhl2 gain-of-function and loss-of-function phenotypes are mainly caused by interference with correct signaling from the forming neural organizing centers (see Fig. 7).

During gastrulation and early neurulation, polarized cell movements from the mesoderm are key regulators in elongating the AP axis of the *Xenopus* embryo (Keller, 2002; Wallingford et al., 2002). Interference with these cell movements can generate defects similar to those we observe by inhibiting Barhl2 activity (Leise and Mueller, 2004), raising the possibility that interference with these cell movements contributes to the Barhl2 loss-of-function phenotype. However, such interference cannot produce an increase in the number of *chordin*- and *shh*-expressing cells, and alteration in apoptosis may secondarily play a part in the convergent extension movements.

Barhl2 could act directly on a survival program or indirectly on a survival pathway

During development, higher animals cells require signals from other cells to avoid apoptosis (reviewed by Raff, 1996). Our data suggest that Barhl2 could act either directly though transcriptional regulation of a cell death program, or indirectly

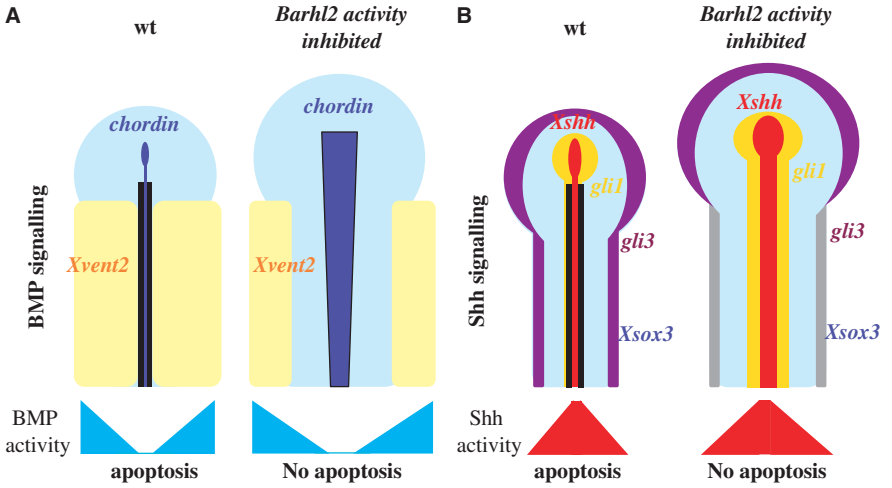

Fig. 7. A model for the role of apoptosis in *Xenopus* neurodevelopment. (A) Mesoderm patterning in wild-type (left panel) or embryos in which apoptosis has been inhibited through *BCL2* or *Xbarhl2AS* injection (right panel). *Chordin* expression is in dark blue. *Xvent2* expression is in light yellow. The neuroectoderm is in blue. The apoptotic area is shown in black. (B) Neuroectodermal patterning in similarly injected embryos. *Xshh* expression is in red. *Gli1* expression is in bright yellow. *Gli3* expression is in violet. *Xsox3* expression is in blue.

through transcriptional modulation of the survival pathways controlling EPCD.

Studies in *C. elegans* and *Drosophila* have demonstrated the importance of transcriptional control of developmental cell death (Kumar and Cakouros, 2004). Hox-dependent regulation of apoptosis, for example, appears to be a conserved mechanism in vertebrate development. Bix3, a *Xenopus* homeobox gene, regulates apoptosis during development, but this activity does not depend on its ability to regulate transcription (Trindade et al., 2003). *Hoxa13* may be involved in eliminating cells located between the forming digits in mice (Stadler et al., 2001), and a direct role for Engrailed genes in the regulation of apoptosis has been suggested in mesencephalic dopaminergic neurons (Alberi et al., 2004). Targeted deletion of *Barhl1,* the closest homologue of *Barhl2* in vertebrates, caused degeneration of mouse cochlear hair cells. Analysis of this phenotype showed that *Barhl1* plays an essential role in the maintenance of cochlear hair cells whereas it had little role in specification and differentiation of these cells (Li et al., 2002). The BH3-only protein, Egl-1, a pro-apoptotic member of the Bcl2 family is transcriptionally controlled in *C. elegans* (Metzstein and Horvitz, 1999). Therefore, *Barhl2* could directly or indirectly regulate the transcription of a gene that encodes a BH3-only protein.

In the neural plate, Shh regulates apoptosis in various ways: it acts as a cell survival signal (Charrier et al., 2001; Chiang et al., 1996; Litingtung and Chiang, 2000), and has a apoptotic promoting activity in chick ventral neuronal precursors and floor-plate cells (Oppenheim et al., 1999). Similarly, several BMPs have been shown to promote apoptosis on developing neural cells (Golden et al., 1999; Mabie et al., 1999). Therefore, *Barhl2* could modulate directly or indirectly the cellular production of these apoptosis-modulating signals and/or their cellular responses, and indirectly control cell survival of the *chordin*- and *shh*-expressing cells. It is foreseeable that determining if this new function is conserved for the fly *barH* and/or for the *ceh-30* and *ceh-31* genes in *C. elegans* would probably help our understanding of *Barhl2* mechanisms of action in vertebrates.

Finally, the main area of expression of *Barhl2* appears to be the dorsal diencephalic primordium**.** Caspase 3-deficient mice exhibit hyperplasia in the diencephalic walls (Kuida et al., 1996), and genetic studies in zebrafish have shown that the dorsal diencephalic domain specifically expands in the absence of BMP signaling (Barth et al., 1999). We observe that the area of *Xpax6* expression at the dorsal diencephalic level is dramatically expanded when Barhl2 activity is inhibited. Further studies are necessary to address the role of *Barhl2* in the anterior neural plate, but it is possible that the *Barhl2* pro-apoptotic function is involved in dorsal diencephalic formation.

In any case, our results argue that a role for Hox proteins as transcriptional regulators of apoptosis and a role for apoptosis in regulating the size of organizing centers appear to be conserved in animal development (Alonso, 2002; Lohmann et al., 2002; Sanz-Ezquerro and Tickle, 2000).

We thank Raphaele Thiebaut, Heithem El-Hodiri, Weeteck Yeo and Jean Gautier for help and advice; Eddy De Robertis, Stephen Ekker, Robert Grainger, Richard Harland, William Harris, V. Hatini, Ali Hemmani Brivanlou, T. Holleman, Paul A. Krieg, A. Lombardo, Francesca Mariani, Randy Moon, Christof Niehrs, Thomas Pieler, Yi Rao, Kenneth Ryan, Yoshiki Sasai, Hazel Sive, Jonathan Slack, Roberto Vignali and Kathy Mahon for gifts of materials; and Martin Raff, Margaret Buckingham and Muriel Perron for their comments on the manuscript. This work was supported by grant from the National Institute of Health (NEI R01 EY12505 and NEI R01 EY12163), the Centre National de la Recherche Scientifique (CNRS – URA 1930) and Association Française contre les Myopathies (grants DdT2002 and DdT2003). B.D. was supported by a Long term European Molecular Biology Organisation Fellowship (EMBO) and by the CNRS.

References

Adams, J. M. (2003). Ways of dying: multiple pathways to apoptosis. *Genes Dev.* **17**, 2481-2495.

Agarwala, S., Sanders, T. A. and Ragsdale, C. W. (2001). Sonic hedgehog control of size and shape in midbrain pattern formation. *Science* **291**, 2147-2150.

Alberi, L., Sgado, P. and Simon, H. H. (2004). Engrailed genes are cell-autonomously required to prevent apoptosis in mesencephalic dopaminergic neurons. *Development* **131**, 3229-3236.

Alonso, C. R. (2002). Hox proteins: sculpting body parts by activating localized cell death. *Curr. Biol.* **12**, R776-R778.

Barlow, A. J. and Francis-West, P. H. (1997). Ectopic application of recombinant BMP-2 and BMP-4 can change patterning of developing chick facial primordia. *Development* **124**, 391-398.

Barth, K. A., Kishimoto, Y., Rohr, K. B., Seydler, C., Schulte-Merker, S. and Wilson, S. W. (1999). Bmp activity establishes a gradient of positional information throughout the entire neural plate. *Development* **126**, 4977-4987.

Britto, J., Tannahill, D. and Keynes, R. (2002). A critical role for sonic hedgehog signaling in the early expansion of the developing brain. *Nat. Neurosci.* **5**, 103-110.

Bulfone, A., Menguzzato, E., Broccoli, V., Marchitiello, A., Gattuso, C., Mariani, M., Consalez, G. G., Martinez, S., Ballabio, A. and Banfi, S. (2000). Barhl1, a gene belonging to a new subfamily of mammalian homeobox genes, is expressed in migrating neurons of the CNS. *Hum. Mol. Genet.* **9**, 1443-1452.

Charrier, J. B., Lapointe, F., le Douarin, N. M. and Teillet, M. A. (2001). Anti-apoptotic role of Sonic hedgehog protein at the early stages of nervous system organogenesis. *Development* **128**, 4011-4020.

Chiang, C., Litingtung, Y., Lee, E., Young, K. E., Corden, J. L., Westphal, H. and Beachy, P. A. (1996). Cyclopia and defective axial patterning in mice lacking Sonic hedgehog gene function. *Nature* **383**, 407-413.

Coffman, C., Harris, W. and Kintner, C. (1990). Xotch, the Xenopus homolog of Drosophila notch. *Science* **249**, 1438-1441.

Dahmane, N., Sanchez, P., Gitton, Y., Palma, V., Sun, T., Beyna, M., Weiner, H. and Ruiz i Altaba, A. (2001). The Sonic Hedgehog-Gli pathway regulates dorsal brain growth and tumorigenesis. *Development* **128**, 5201-5212.

Dale, L. and Jones, C. M. (1999). BMP signalling in early Xenopus development. *BioEssays* **21**, 751-760.

de la Rosa, E. J. and de Pablo, F. (2000). Cell death in early neural development: beyond the neurotrophic theory. *Trends Neurosci.* **23**, 454-458.

Edelman, D. B., Meech, R. and Jones, F. S. (2000). The homeodomain protein Barx2 contains activator and repressor domains and interacts with members of the CREB family. *J. Biol. Chem.* **275**, 21737-21745.

Ekker, S. C., McGrew, L. L., Lai, C. J., Lee, J. J., von Kessler, D. P., Moon, R. T. and Beachy, P. A. (1995). Distinct expression and shared activities of members of the hedgehog gene family of Xenopus laevis. *Development* **121**, 2337-2347.

Gamse, J. and Sive, H. (2000). Vertebrate anteroposterior patterning: the Xenopus neurectoderm as a paradigm. *BioEssays* **22**, 976-986.

Golden, J. A., Bracilovic, A., McFadden, K. A., Beesley, J. S., Rubenstein, J. L. and Grinspan, J. B. (1999). Ectopic bone morphogenetic proteins 5 and 4 in the chicken forebrain lead to cyclopia and holoprosencephaly. *Proc. Natl. Acad. Sci. USA* **96**, 2439-2444.

Harland, R. M. (1991). In situ hybridization: an improved whole-mount method for Xenopus embryos. *Methods Cell Biol.* **36**, 685-695.

Harris, W. A. and Hartenstein, V. (1991). Neuronal determination without cell division in Xenopus embryos. *Neuron* **6**, 499-515.

Hensey, C. and Gautier, J. (1998). Programmed cell death during Xenopus development: a spatio-temporal analysis. *Dev. Biol.* **203**, 36-48.
Higashijima, S., Kojima, T., Michiue, T., Ishimaru, S., Emori, Y. and Saigo, K. (1992). Dual Bar homeo box genes of Drosophila required in two photoreceptor cells, R1 and R6, and primary pigment cells for normal eye development. *Genes Dev.* **6**, 50-60.
Hirsch, N. and Harris, W. A. (1997). Xenopus Pax-6 and retinal development. *J. Neurobiol.* **32**, 45-61.
Hjalt, T. A. and Murray, J. C. (1999). The human BARX2 gene: genomic structure, chromosomal localization, and single nucleotide polymorphisms. *Genomics* **62**, 456-459.
Jacob, J., Briscoe, J., Britto, J., Tannahill, D. and Keynes, R. (2003). Gli proteins and the control of spinal-cord patterning. *EMBO Rep.* **4**, 761-765.
Jacobson, M. D., Weil, M. and Raff, M. C. (1997). Programmed cell death in animal development. *Cell* **88**, 347-354.
Jamrich, M., Sargent, T. D. and Dawid, I. B. (1987). Cell-type-specific expression of epidermal cytokeratin genes during gastrulation of Xenopus laevis. *Genes Dev.* **1**, 124-132.
Jaynes, J. B. and O'Farrell, P. H. (1991). Active repression of transcription by the engrailed homeodomain protein. *EMBO J.* **10**, 1427-1433.
Joubin, K. and Stern, C. D. (2001). Formation and maintenance of the organizer among the vertebrates. *Int. J. Dev. Biol.* **45**, 165-175.
Keller, R. (2002). Shaping the vertebrate body plan by polarized embryonic cell movements. *Science* **298**, 1950-1954.
Kiecker, C. and Niehrs, C. (2001). A morphogen gradient of Wnt/beta-catenin signalling regulates anteroposterior neural patterning in Xenopus. *Development* **128**, 4189-4201.
Kojima, T., Sato, M. and Saigo, K. (2000). Formation and specification of distal leg segments in Drosophila by dual Bar homeobox genes, BarH1 and BarH2. *Development* **127**, 769-778.
Kuan, C. Y., Roth, K. A., Flavell, R. A. and Rakic, P. (2000). Mechanisms of programmed cell death in the developing brain. *Trends Neurosci.* **23**, 291-297.
Kuida, K., Zheng, T. S., Na, S., Kuan, C., Yang, D., Karasuyama, H., Rakic, P. and Flavell, R. A. (1996). Decreased apoptosis in the brain and premature lethality in CPP32-deficient mice. *Nature* **384**, 368-372.
Kumar, S. and Cakouros, D. (2004). Transcriptional control of the core cell-death machinery. *Trends Biochem. Sci.* **29**, 193-199.
Lee, K. J., Dietrich, P. and Jessell, T. M. (2000). Genetic ablation reveals that the roof plate is essential for dorsal interneuron specification. *Nature* **403**, 734-740.
Leise, W. F., 3rd and Mueller, P. R. (2004). Inhibition of the cell cycle is required for convergent extension of the paraxial mesoderm during Xenopus neurulation. *Development* **131**, 1703-1715.
Li, S., Price, S. M., Cahill, H., Ryugo, D. K., Shen, M. M. and Xiang, M. (2002). Hearing loss caused by progressive degeneration of cochlear hair cells in mice deficient for the Barhl1 homeobox gene. *Development* **129**, 3523-3532.
Lim, J. and Choi, K. W. (2003). Bar homeodomain proteins are anti-proneural in the Drosophila eye: transcriptional repression of atonal by Bar prevents ectopic retinal neurogenesis. *Development* **130**, 5965-5974.
Litingtung, Y. and Chiang, C. (2000). Specification of ventral neuron types is mediated by an antagonistic interaction between Shh and Gli3. *Nat. Neurosci.* **3**, 979-985.
Lohmann, I., McGinnis, N., Bodmer, M. and McGinnis, W. (2002). The Drosophila Hox gene deformed sculpts head morphology via direct regulation of the apoptosis activator reaper. *Cell* **110**, 457-466.
Mabie, P. C., Mehler, M. F. and Kessler, J. A. (1999). Multiple roles of bone morphogenetic protein signaling in the regulation of cortical cell number and phenotype. *J. Neurosci.* **19**, 7077-7088.
Metzstein, M. M. and Horvitz, H. R. (1999). The C. elegans cell death specification gene ces-1 encodes a snail family zinc finger protein. *Mol. Cell* **4**, 309-319.
Mo, Z., Li, S., Yang, X. and Xiang, M. (2004). Role of the Barhl2 homeobox gene in the specification of glycinergic amacrine cells. *Development* **131**, 1607-1618.
Muhr, J., Andersson, E., Persson, M., Jessell, T. M. and Ericson, J. (2001). Groucho-mediated transcriptional repression establishes progenitor cell pattern and neuronal fate in the ventral neural tube. *Cell* **104**, 861-873.
Munoz-Sanjuan, I. and Brivanlou, A. H. (2002). Neural induction, the default model and embryonic stem cells. *Nat. Rev. Neurosci.* **3**, 271-280.
Newport, J. and Dasso, M. (1989). On the coupling between DNA replication and mitosis. *J. Cell Sci. Suppl.* **12**, 149-160.
Niehrs, C. (2004). Regionally specific induction by the Spemann-Mangold organizer. *Nat. Rev. Genet.* **5**, 425-434.
Nieuwkoop, P. D. and Faber, J. (1967). *Normal Table of* Xenopus laevis *(Daudin)*. Amsterdam, The Netherlands: Elsevier/North Holland Publishing.
Onichtchouk, D., Gawantka, V., Dosch, R., Delius, H., Hirschfeld, K., Blumenstock, C. and Niehrs, C. (1996). The Xvent-2 homeobox gene is part of the BMP-4 signalling pathway controlling [correction of controling] dorsoventral patterning of Xenopus mesoderm. *Development* **122**, 3045-3053.
Oppenheim, R. W., Homma, S., Marti, E., Prevette, D., Wang, S., Yaginuma, H. and McMahon, A. P. (1999). Modulation of early but not later stages of programmed cell death in embryonic avian spinal cord by sonic hedgehog. *Mol. Cell. Neurosci.* **13**, 348-361.
Patterson, K., Cleaver, O., Gerber, W., White, F. and Krieg, P. (2000). Distinct expression pattern of two *Xenopus* Bar homeobox genes. *Dev. Genes Evol.* **210**, 140-144.
Penzel, R., Oschwald, R., Chen, Y., Tacke, L. and Grunz, H. (1997). Characterization and early embryonic expression of a neural specific transcription factor xSOX3 in Xenopus laevis. *Int. J. Dev. Biol.* **41**, 667-677.
Poggi, L., Vottari, T., Barsacchi, G., Wittbrodt, J. and Vignali, R. (2004). The homeobox gene XBh1 cooperates with proneural genes to specify ganglion cell fate within the Xenopus neural retina. *Development* **131**, 2305-2315.
Puelles, L. and Rubenstein, J. L. (2003). Forebrain gene expression domains and the evolving prosomeric model. *Trends Neurosci.* **26**, 469-476.
Raff, M. (1996). Size control: the regulation of cell numbers in animal development. *Cell* **86**, 173-175.
Rubenstein, J. L., Shimamura, K., Martinez, S. and Puelles, L. (1998). Regionalization of the prosencephalic neural plate. *Annu. Rev. Neurosci.* **21**, 445-477.
Ruiz i Altaba, A., Nguyen, V. and Palma, V. (2003). The emergent design of the neural tube: prepattern, SHH morphogen and GLI code. *Curr. Opin. Genet. Dev.* **13**, 513-521.
Saba, R., Nakatsuji, N. and Saito, T. (2003). Mammalian BarH1 confers commissural neuron identity on dorsal cells in the spinal cord. *J. Neurosci.* **23**, 1987-1991.
Saito, T., Sawamoto, K., Okano, H., Anderson, D. J. and Mikoshiba, K. (1998). Mammalian BarH homologue is a potential regulator of neural bHLH genes. *Dev. Biol.* **199**, 216-225.
Saka, Y. and Smith, J. C. (2001). Spatial and temporal patterns of cell division during early Xenopus embryogenesis. *Dev. Biol.* **229**, 307-318.
Sanz-Ezquerro, J. J. and Tickle, C. (2000). Autoregulation of Shh expression and Shh induction of cell death suggest a mechanism for modulating polarising activity during chick limb development. *Development* **127**, 4811-4823.
Sasai, Y., Lu, B., Steinbeisser, H., Geissert, D., Gont, L. K. and de Robertis, E. M. (1994). Xenopus chordin: a novel dorsalizing factor activated by organizer-specific homeobox genes. *Cell* **79**, 779-790.
Sato, M., Kojima, T., Michiue, T. and Saigo, K. (1999). Bar homeobox genes are latitudinal prepattern genes in the developing Drosophila notum whose expression is regulated by the concerted functions of decapentaplegic and wingless. *Development* **126**, 1457-1466.
Schier, A. F. and Sive, H. (2001). Axis formation and patterning in zebrafish. *Curr. Opin. Genet. Dev.* **11**, 393-404.
Smith, S. T. and Jaynes, J. B. (1996). A conserved region of engrailed, shared among all en-, gsc-, Nk1-, Nk2- and msh-class homeoproteins, mediates active transcriptional repression in vivo. *Development* **122**, 3141-3150.
Stadler, H. S., Higgins, K. M. and Capecchi, M. R. (2001). Loss of Eph-receptor expression correlates with loss of cell adhesion and chondrogenic capacity in Hoxa13 mutant limbs. *Development* **128**, 4177-4188.
Stern, C. D. (2002). Induction and initial patterning of the nervous system – the chick embryo enters the scene. *Curr. Opin. Genet. Dev.* **12**, 447-451.
Thibert, C., Teillet, M. A., Lapointe, F., Mazelin, L., le Douarin, N. M. and Mehlen, P. (2003). Inhibition of neuroepithelial patched-induced apoptosis by sonic hedgehog. *Science* **301**, 843-846.
Trindade, M., Messenger, N., Papin, C., Grimmer, D., Fairclough, L., Tada, M. and Smith, J. C. (2003). Regulation of apoptosis in theXenopus embryo by Bix3. *Development* **130**, 4611-4622.
Turner, D. L. and Weintraub, H. (1994). Expression of achaete-scute homolog 3 in Xenopus embryos converts ectodermal cells to a neural fate. *Genes Dev.* **8**, 1434-1447.
Veenstra, G. J., Peterson-Maduro, J., Mathu, M. T., van der Vliet, P. C. and Destree, O. H. (1998). Non-cell autonomous induction of apoptosis

and loss of posterior structures by activation domain-specific interactions of Oct-1 in the Xenopus embryo. *Cell Death Differ.* **5**, 774-784.

Wallace, V. A. (1999). Purkinje-cell-derived Sonic hedgehog regulates granule neuron precursor cell proliferation in the developing mouse cerebellum. *Curr. Biol.* **9**, 445-448.

Wallingford, J. B., Fraser, S. E. and Harland, R. M. (2002). Convergent extension: the molecular control of polarized cell movement during embryonic development. *Dev. Cell* **2**, 695-706.

Wilson, S. I. and Edlund, T. (2001). Neural induction: toward a unifying mechanism. *Nat. Neurosci. Suppl.* **4**, 1161-1168.

Yeo, W. and Gautier, J. (2003). A role for programmed cell death during early neurogenesis in xenopus. *Dev. Biol.* **260**, 31-45.

Yeo, W. and Gautier, J. (2004). Early neural cell death: dying to become neurons. *Dev. Biol.* **274**, 233-244.